

# Oxidation of Buckminsterfullerene with *m*-Chloroperoxybenzoic Acid. Characterization of a C<sub>s</sub> Isomer of the Diepoxide C<sub>60</sub>O<sub>2</sub>

Alan L. Balch,\* David A. Costa, Bruce C. Noll, and Marilyn M. Olmstead

Contribution from the Department of Chemistry, University of California, Davis, California 95616

Received March 28, 1995<sup>⊗</sup>

**Abstract:** In order to assess the oxidative stability of C<sub>60</sub> and to prepare precursors of fullerene polymerization, the products that are obtained by the oxidation of C<sub>60</sub> with *m*-chloroperoxybenzoic acid have been compared with those produced by photooxygenation or by ozonolysis. A wider and more readily handled set of products are obtained by the *m*-chloroperoxybenzoic acid oxidation. All three processes produce the previously characterized epoxide. The *m*-chloroperoxybenzoic acid oxidation produces sufficient quantities of the higher oxide C<sub>60</sub>O<sub>2</sub> so that it has been structurally characterized. The <sup>13</sup>C NMR spectrum of C<sub>60</sub>O<sub>2</sub> indicates that the sample is isomerically pure and that it is one of three possible isomers with C<sub>s</sub> symmetry. C<sub>60</sub>O<sub>2</sub> reacts with Ir(CO)Cl(PPh<sub>3</sub>)<sub>2</sub> to form black crystals of (η<sup>2</sup>-C<sub>60</sub>O<sub>2</sub>)Ir(CO)Cl(PPh<sub>3</sub>)<sub>2</sub>·5C<sub>6</sub>H<sub>6</sub>. A structure determination by X-ray diffraction shows that the structure consists of the fullerene bound to the iridium complex in the expected η<sup>2</sup> fashion, but that the oxygen atoms are disordered over seven sites of varying occupancy. Additionally there is exchange disorder that involves the carbon monoxide and chloride ligands. Despite these problems, the structure can be analyzed to give information on the structure of this isomer of C<sub>60</sub>O<sub>2</sub>. This dioxide is a fullerene diepoxide with both oxygen atoms positioned over 6:6 ring junctions on a common six-membered face of the carbon cage. Contrary to some earlier experimental and theoretical work, the fullerene core has resisted rupture in the oxidative process that forms this dioxide.

## Introduction

The reactivity of the fullerenes,<sup>1</sup> and C<sub>60</sub> in particular, toward dioxygen and other oxidizing agents is likely to be an important consideration in any technological application of these substances. We have observed that prolonged storage of purple toluene solutions of C<sub>60</sub> in air is accompanied by a gradual color change to brown with the concomitant formation of an amorphous tan solid. This solid is presumed to be polymeric since it does not dissolve in any common organic solvents. There have been a number of studies of the oxidation of C<sub>60</sub>, and so far the monooxide, C<sub>60</sub>O, is the best characterized oxidation product. C<sub>60</sub>O has been obtained by a number of oxidation processes in solution. These include photooxygenation of C<sub>60</sub>,<sup>2,3</sup> electrochemical oxidation of C<sub>60</sub>,<sup>4</sup> addition of dimethyldioxirane to C<sub>60</sub>,<sup>5</sup> and ozonolysis of C<sub>60</sub>.<sup>6,7</sup> This fullerene oxide is also formed as a byproduct during fullerene synthesis.<sup>2,3</sup> Several geometric arrangements for C<sub>60</sub>O, including an epoxide and an

oxido annulene structure in which the oxygen atom would sit over a 6:6 ring junction of the fullerene, and an isomer with the oxygen atom placed above a 5:6 ring junction, have been proposed for C<sub>60</sub>O.<sup>3,8–10</sup> However, the <sup>13</sup>C NMR spectrum<sup>3,5</sup> and the X-ray crystallographic data on an organometallic derivative<sup>11</sup> indicate that the C<sub>60</sub>O that has been isolated has an epoxide structure with the oxygen atom located over a 6:6 ring junction. Higher oxides, C<sub>60</sub>O<sub>n</sub> with *n* = 2, 3, 4, 5, etc., have also been reported to form during photooxygenation,<sup>2</sup> electrochemical oxidation,<sup>4</sup> and ozonolysis<sup>6</sup> of C<sub>60</sub> in solution. For these higher fullerene oxides much less information regarding their structures and isomeric purities is known. For C<sub>60</sub>O<sub>2</sub> theoretical calculations have predicted that the most stable structure results in breaking of a C–C bond with the oxygen incorporated into a carbonyl–oxide unit.<sup>9</sup>

The oxidation of solid C<sub>60</sub>, generally in the form of thin films, has also been investigated.<sup>12–14</sup> Photooxygenation of thin C<sub>60</sub> films results in the formation carbon monoxide, carbon dioxide, and carbonyl-containing species. In particular, one study suggested that photooxygenation resulted in cage opening to form C<sub>60</sub>O<sub>2</sub> with the rupture of the carbon–carbon bond at a 5:6 ring junction and the formation of two keto functions at that site.<sup>13</sup>

The fullerene oxide, C<sub>60</sub>O, is an interesting starting material for the formation of other fullerene-based entities. It has been

<sup>⊗</sup> Abstract published in *Advance ACS Abstracts*, August 1, 1995.

(1) For reviews on fullerene preparation and chemistry see: *Acc. Chem. Res.* **1992**, 25, Special Issue 3. *Fullerenes: Synthesis, Properties, and Chemistry of Large Carbon Clusters*; Hammond, G. S., Kuck, V. J., Eds.; ACS Symposium Series 481; American Chemical Society: Washington, DC, 1992. Taylor, R.; Walton, D. R. M. *Nature* **1993**, 363, 685. *New Directions in the Chemistry and Physics of Fullerenes*; Kadish, K., Rouff, R., Eds.; The Electrochemical Society.

(2) Wood, J. M.; Kahr, B.; Hake, S. H., II; Dejarne, L.; Cooks, R. G.; Ben-Amotz, D. *J. Am. Chem. Soc.* **1991**, 113, 5907.

(3) Creegan, K. M.; Robbins, J. L.; Robbins, W. K.; Millar, J. M.; Sherwood, R. D.; Tindall, P. J.; Cox, D. M.; Smith, A. B., III; McCauley, J. P., Jr.; Jones, D. R.; Gallagher, R. T. *J. Am. Chem. Soc.* **1992**, 114, 1103. Millar, J. M.; Creegan, K. M.; Robbins, J. L.; Robbins, W. K.; Sherwood, R. D.; Tindall, P. J.; Cox, D. M. *Synth. Met.* **1993**, 59, 317.

(4) Kalsbeck, W. A.; Thorp, H. H. *J. Electroanal. Chem.* **1991**, 314, 363.

(5) Elemen, Y.; Silverman, S. K.; Sheu, C.; Kao, M.; Foote, C. S.; Alvarez, M. M.; Whetten, R. L. *Angew. Chem., Int. Ed. Engl.* **1992**, 31, 351.

(6) Heymann, D.; Chibante, L. P. F. *Chem. Phys. Lett.* **1993**, 207, 339.

(7) Malhotra, R.; Kumar, S.; Satyam, A. *J. Chem. Soc., Chem. Commun.* **1994**, 1339.

(8) Raghavachari, K. *Int. J. Mod. Phys. B* **1992**, 6, 3821. Ravhavachari, K. *Chem. Phys. Lett.* **1992**, 195, 221.

(9) Menon, M.; Sunbaswamy, K. R. *Chem. Phys. Lett.* **1993**, 201, 321.

(10) Raghavachari, K.; Sosa, C. *Chem. Phys. Lett.* **1993**, 209, 223.

(11) Balch, A. L.; Costa, D. A.; Lee, J. W.; Noll, B. C.; Olmstead, M. M. *Inorg. Chem.* **1994**, 33, 2071.

(12) Kroll, G. H.; Benning, P. J.; Chen, Y.; Ohno, T. R.; Weaver, J. H.; Chibante, L. P. F.; Smalley, R. E. *Chem. Phys. Lett.* **1991**, 181, 112.

(13) Taliani, C.; Ruani, G.; Zamboni, R.; Danieli, R.; Rossini, S.; Denisov, V. N.; Burlakov, V. M.; Negri, F.; Orlandi, G.; Zerbetto, F. *J. Chem. Soc., Chem. Commun.* **1993**, 220.

(14) Werner, H.; Schedel-Niedrig, Th.; Wohlers, M.; Herein, D.; Herzog, B.; Schlögl, R.; Keil, M.; Bradshaw, A. M.; Kirshner, J. *J. Chem. Soc., Faraday Trans.* **1994**, 90, 403.

shown to be a precursor for the formation of tough, brown films that can be grown on a variety of electrode surfaces by electrochemical reduction of solutions of the epoxide.<sup>15</sup> These films are electrochemically active and appear to be conducting since they can be imaged by scanning tunneling microscopy. Mass spectroscopic studies have shown that C<sub>60</sub>O is a starting material for the formation of odd-numbered fullerene-like species including enlarged ions, C<sub>119</sub><sup>-</sup>, C<sub>129</sub><sup>-</sup>, and C<sub>139</sub><sup>-</sup>, and the fragmented ions, C<sub>59</sub><sup>-</sup>, C<sub>57</sub><sup>-</sup>, C<sub>55</sub><sup>-</sup>, and C<sub>53</sub><sup>-</sup>.<sup>16-18</sup>

In order to provide routes to the preparation of the higher fullerene oxides, especially as precursors for electrochemical film growth, we have undertaken a study of fullerene oxidation with *m*-chloroperoxybenzoic acid and compared this oxidation process with the previously reported photooxygenations and ozonolysis. This work has led to the production of suitable amounts of C<sub>60</sub>O<sub>2</sub> in isomerically pure form to allow us to structurally characterize this material. Thorough structural characterization of fullerenes can be a difficult task. Even if isomerically pure samples can be obtained, spectroscopic techniques such as <sup>13</sup>C NMR spectroscopy can only yield the symmetry of the compound but frequently cannot differentiate between isomers of the same symmetry. X-ray crystallography, while definitive for many organic molecules, is complicated in the case of fullerenes by the frequent presence of orientational disorder within the solid. For example, both C<sub>60</sub> and C<sub>60</sub>O form isomorphous crystals with the latter displaying orientational disorder in the location of the epoxide functionality.<sup>19,20</sup>

Reaction of fullerenes (C<sub>60</sub>, C<sub>70</sub>, C<sub>84</sub>) and their derivatives (i.e. C<sub>60</sub>O) with Vaska's complex, Ir(CO)Cl(PPh<sub>3</sub>)<sub>2</sub>, results in the formation of crystalline adducts which can be characterized by single-crystal X-ray diffraction.<sup>11,21-23</sup> This procedure represents a structural probe that allows the fullerene or fullerene derivative to be obtained in sufficiently ordered form so that geometric information can be realized. The formation of these adducts is a readily reversible process, and the act of crystallization results in separation of the least soluble adduct.<sup>24</sup>

## Results

**Synthetic Studies.** The reaction of C<sub>60</sub> with *m*-chloroperoxybenzoic acid has been examined under a variety of conditions. Treatment of C<sub>60</sub> with a 10-fold molar excess of *m*-chloroperoxybenzoic acid in toluene/dichloromethane at 80 °C for 12 h produces a brown solution and a brown precipitate which does not dissolve in common organic solvents. Analysis of the solution by high-pressure liquid chromatography (HPLC) with a Buckyclutcher column<sup>25</sup> gives the profile shown in Trace A of Figure 1. Seven clearly separated peaks are present. Unreacted C<sub>60</sub> and the known epoxide, C<sub>60</sub>O, are the first two substances to elute, and these are obtained in 40 and 15% yield,

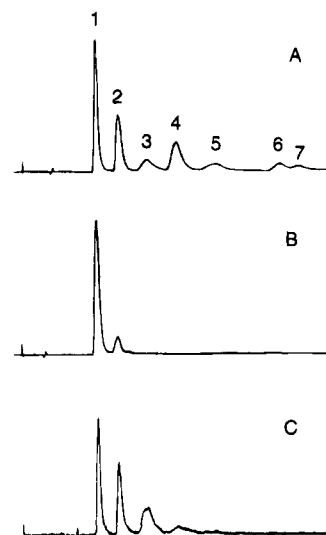


**Figure 1.** High-pressure liquid chromatography (HPLC) profiles (Buckyclutcher-1, toluene, 600 nm visible detection) for the products of (A) *m*-chloroperoxybenzoic acid oxidation of C<sub>60</sub>, (B) photosensitized oxidation of C<sub>60</sub> by dioxygen, and (C) ozonolysis of C<sub>60</sub>.

respectively. The epoxide, C<sub>60</sub>O, has been identified via comparison of its UV/vis and <sup>13</sup>C NMR spectra with previous reports<sup>3,5</sup> and through X-ray crystallographic examination of its complex with Ir(CO)Cl(PPh<sub>3</sub>)<sub>2</sub>.<sup>11</sup> Five additional peaks (3-7) are also present. Analysis of isolated samples from peaks 3 and 4 by electron impact mass spectrometry shows similar spectra with a strong parent ion at 752 amu and fragment peaks at 736 and 720 amu. Thus both are formulated as dioxides, C<sub>60</sub>O<sub>2</sub>. Using this procedure an 8% yield of C<sub>60</sub>O<sub>2</sub> from peak 4 (compound 4) can be isolated. This set of conditions maximizes the production of the range of oxidation products that are contained in peaks 3-7. However, a considerable amount of the fullerene is lost as the brown precipitate. The conditions given in the Experimental Section produce C<sub>60</sub>O and C<sub>60</sub>O<sub>2</sub> in 30% and 8% yield, respectively, while allowing C<sub>60</sub> itself to be recovered in 60% yield.

The products obtained by *m*-chloroperoxybenzoic acid oxidation of C<sub>60</sub> have been compared with those produced by two other oxidation procedures: photooxidation with dioxygen<sup>3</sup> and ozonolysis.<sup>6,7</sup> Trace B of Figure 2 shows the HPLC profile of a sample of C<sub>60</sub> that was prepared by photooxidation with dioxygen in the presence of benzil as sensitizer. Peaks due to unreacted C<sub>60</sub> and the epoxide C<sub>60</sub>O are present, but the five additional products that are seen in the *m*-chloroperoxybenzoic acid oxidation are absent. Trace C of Figure 2 shows the HPLC profile that was obtained from a toluene solution of C<sub>60</sub> that had been treated with an ozone/dioxygen mixture. This procedure produces an unstable amber solution from which a yellow-brown amorphous solid slowly precipitates. Analysis of the toluene solution reveals that the soluble products that correspond to those seen in the *m*-chloroperoxybenzoic acid oxidation are present but that the relative yields of individual species are different. Because of the problem of continual precipitation of the amorphous yellow-brown powder from these solutions, ozonolysis does not appear to be an attractive means of generating the oxidation products.

A sufficient quantity of the material contained in peak 4 (compound 4) from the *m*-chloroperoxybenzoic acid oxidation has been collected to allow thorough structural analysis.<sup>26</sup> Compound 4 has been isolated as a brown powder which has

(15) Fedurco, M.; Costa, D.; Balch, A. L.; Fawcett, W. R. *Angew. Chem.* **1995**, *34*, 194.

(16) McElvany, S. W.; Callahan, J. H.; Ross, M. M.; Lamb, L. D.; Huffman, D. R. *Science* **1993**, *260*, 1632.

(17) Deng, J.-P.; Ju, D. D.; Her, G.-R.; Mou, C.-Y.; Chen, C.-J.; Lin, Y.-Y.; Han, C.-C. *J. Phys. Chem.* **1993**, *97*, 11575.

(18) Taylor, R. *J. Chem. Soc., Chem. Commun.* **1994**, 1629.

(19) Vaughan, G. B. M.; Heiney, P. A.; Cox, D. E.; McGhie, A. R.; Jones, D. R.; Strongin, R. M.; Cichy, M. A.; Smith, A. B., III. *Chem. Phys.* **1992**, *168*, 185.

(20) Buerigi, H. B.; Blanc, E.; Schwarzenbach, D.; Liu, S.; Lu, Y. J.; Kappes, M. M.; Ibers, J. A. *Angew. Chem., Int. Ed. Engl.* **1992**, *31*, 640.

(21) Balch, A. L.; Catalano, V. J.; Lee, J. W. *Inorg. Chem.* **1991**, *30*, 3980.

(22) Balch, A. L.; Catalano, V. J.; Lee, J. W.; Olmstead, M. M.; Parkin, S. R. *J. Am. Chem. Soc.* **1991**, *113*, 8953.

(23) Balch, A. L.; Ginwalla, A. S.; Lee, J. W.; Noll, B. C.; Olmstead, M. M. *J. Am. Chem. Soc.* **1994**, *116*, 2227.

(24) Balch, A. L.; Lee, J. W.; Noll, B. C.; Olmstead, M. M. *Inorg. Chem.* **1994**, *33*, 5238.

(25) Welch, C. J.; Pirkle, W. H. *J. Chromatogr.* **1992**, *609*, 89.

(26) We have also collected a sample of the material from peak 3 but have been unable to obtain a <sup>13</sup>C NMR spectrum from it. We suspect that this peak may consist of several isomers of C<sub>60</sub>O<sub>2</sub>.

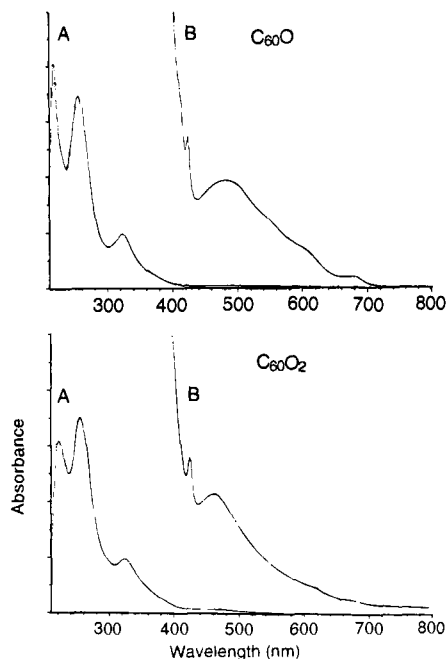


**Figure 2.** The UV/vis absorption spectrum of **4**,  $C_{60}O_2$  and  $C_{60}O$  in (A) hexane and (B) toluene.

solubility in organic solvents that is similar to that of  $C_{60}$ . It is most soluble in carbon disulfide and *o*-dichlorobenzene, less soluble in toluene and benzene, and only slightly soluble (but more soluble than  $C_{60}$ ) in dichloromethane. These solutions are yellow.

**Spectroscopic Studies on **4**,  $C_{60}O_2$ .** The UV/vis absorption spectrum of **4** is shown in Figure 2. The visible portion consists of a broad band at 466 nm and sharper absorption at 424 nm. The broad band is blue-shifted relative to its counterpart in the spectrum of  $C_{60}O$  ( $\lambda_{max}$  496 and 424). In the UV region, the spectrum shows the three typical fullerene absorptions ( $\lambda_{max}$  = 238, 254, and 324 nm).

The infrared spectrum of **4** in a KBr matrix reveals no bands above  $1450\text{ cm}^{-1}$ . Thus no C–H or C=O units are present. Fullerene-like,<sup>27</sup> but broadened, bands are seen at  $1429.0$  and  $1182.1\text{ cm}^{-1}$ . The region from  $806$  to  $480\text{ cm}^{-1}$  is complex with at least 20 bands discernible. Of these the band at  $526.5\text{ cm}^{-1}$  dominates the entire spectrum, and there is an intense cluster of absorbances at about  $788\text{ cm}^{-1}$ .

The  $^{13}\text{C}$  NMR spectrum of **4** in carbon disulfide solution with chromium(III) tris(acetylacetonate) as a relaxation reagent is shown in Figure 3. The two upfield resonances at 82.3 and 78.4 ppm are assigned to the carbon atoms in epoxide units. For comparison,  $C_{60}O$  has a single resonance at 90.18 ppm that is in this upfield region.<sup>3</sup> The remaining resonances occur in the fullerene cage region, 150–139 ppm. Four of these (those at 147.7, 143.2, 141.3, and 140.0 ppm) have intensities that are approximately one-half of the intensities of the remaining individual resonances. Twenty-five additional resonances are observed with the one at 144.21 ppm representing two accidentally degenerate resonances. These data define the symmetry of this fullerene dioxide and show that it has been obtained in isometrically pure form. If this compound is a diepoxide with both oxygen atoms lying across 6:6 ring junctions, then there are eight possible regioisomers that can exist as shown in Figure 4. This figure also shows the symmetry

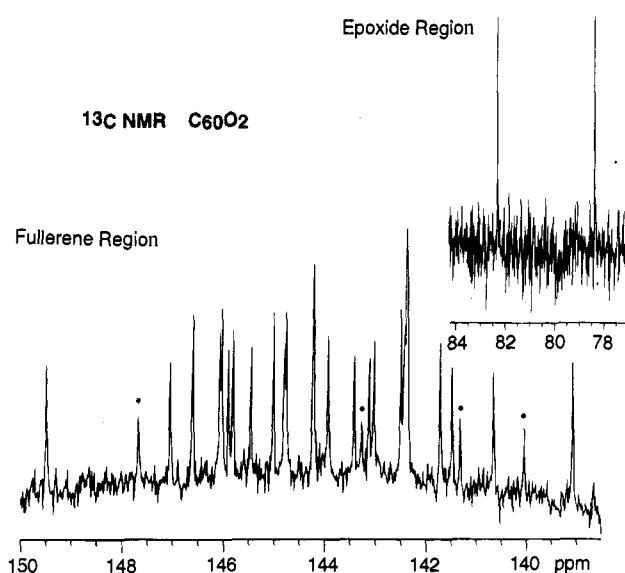


**Figure 3.** The  $^{13}\text{C}$  NMR spectrum of  $C_{60}O_2$ , **4**, in carbon disulfide solution with  $\text{Cr}(\text{acetylacetonate})_3$  as a relaxation reagent. The four peaks of relative intensity 1 in the fullerene region are denoted by an asterisk.

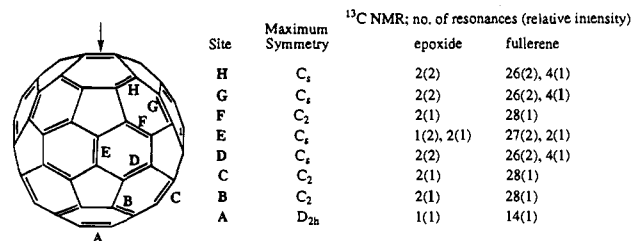


**Figure 4.** Structures for  $C_{60}O_2$  as a diepoxide. The eight possible regioisomers that can arise by double addition at 6:6 ring junctions in  $C_{60}$  and their symmetry. The site of the first addition is indicated by the arrow and the letters A–H indicate the site of the second addition.

of each isomer and the pattern of resonances that are predicted to occur in the  $^{13}\text{C}$  NMR spectrum of each isomer. The pattern of resonances shown in Figure 3, with two resonances in the epoxide region and four resonances with approximately half the intensity of the others in the fullerene cage region, is consistent with **4** being one of the three isomers, D, G, and H, with  $C_2$  symmetry. Figure 5 shows drawings of each of these three isomers from a common perspective.

**Reaction of  $C_{60}O_2$  with  $\text{Ir}(\text{CO})\text{Cl}(\text{PPh}_3)_2$  and Crystallographic Characterization of  $(\eta^2-C_{60}O_2)\text{Ir}(\text{CO})\text{Cl}(\text{PPh}_3)_2 \cdot 5\text{C}_6\text{H}_6$ .** Treatment of  $C_{60}O_2$ , **4**, with  $\text{Ir}(\text{CO})\text{Cl}(\text{PPh}_3)_2$  in benzene results in formation of a black crystalline solid which can be isolated in 50% yield. The infrared spectrum of the single crystal that was used for X-ray data collection showed carbon monoxide stretching vibrations at 2035, 2025, and  $1994\text{ cm}^{-1}$ . The increase in these values over that of the parent,  $\text{Ir}(\text{CO})\text{Cl}(\text{PPh}_3)_2$  at  $1959\text{ cm}^{-1}$ , is indicative of adduct formation. The observation of three carbon monoxide stretching vibrations is consistent with the X-ray diffraction data which indicate that a set of isomeric adducts co-crystallize.<sup>21–24,28</sup>

Crystals of  $(\eta^2-C_{60}O_2)\text{Ir}(\text{CO})\text{Cl}(\text{PPh}_3)_2 \cdot 5\text{C}_6\text{H}_6$  are isostructural with those of  $(\eta^2-C_{60})\text{Ir}(\text{CO})\text{Cl}(\text{PPh}_3)_2 \cdot 5\text{C}_6\text{H}_6$ <sup>21</sup> and of  $(\eta^2-C_{60}O)\text{Ir}(\text{CO})\text{Cl}(\text{PPh}_3)_2 \cdot 0.53\text{CHCl}_3 \cdot 4.47\text{C}_6\text{H}_6$ .<sup>24</sup> Figure 5 shows a drawing of the fullerene adduct. Some selected interatomic distances and angles are given in Table 1. As in  $(\eta^2-C_{60})\text{Ir}(\text{CO})\text{Cl}(\text{PPh}_3)_2$  and  $(\eta^2-C_{60}O)\text{Ir}(\text{CO})\text{Cl}(\text{PPh}_3)_2$  the iridium atom is coordinated to the fullerene through the olefinic carbon–carbon bond at a 6:6 ring junction, and the orientations of the

(27) Cox, D. M.; Behal, S.; Disko, M.; Gorun, S. M.; Greaney, M.; Hsu, C. S.; Kollin, E. B.; Millar, J.; Robbins, J.; Robbins, W.; Sherwood, R. D.; Tindall, P. *J. Am. Chem. Soc.* **1991**, *113*, 2940.

(28) Vaska, L. *Acc. Chem. Res.* **1968**, *1*, 335.

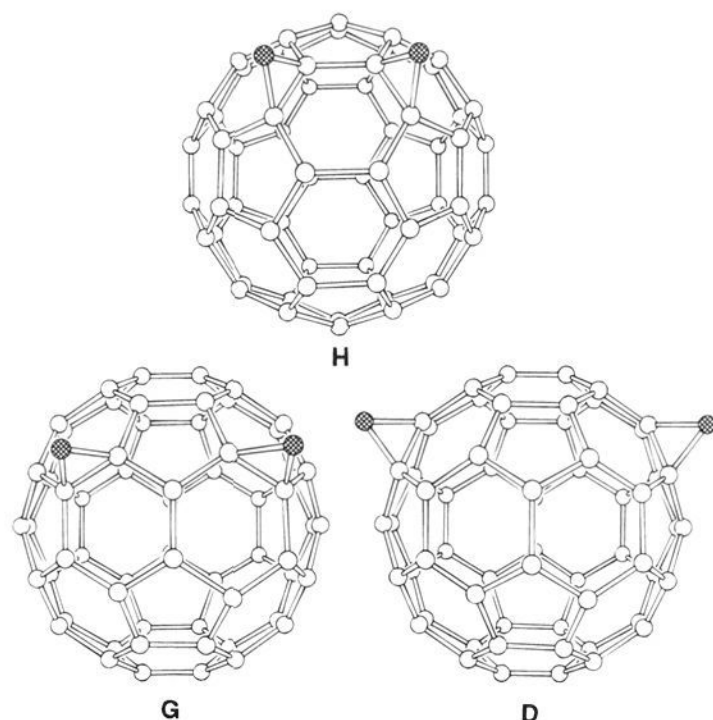


**Figure 5.** Drawings of the three isomers, **D**, **G**, and **H**, of  $C_{60}O_2$  with  $C_s$  symmetry from a common perspective with the mirror plane perpendicular to the page.

**Table 1.** Selected Bond Distances and Angles in  $(\eta^2-C_{60}O_2)Ir(CO)Cl(PPh_3)_2 \cdot 5C_6H_6$

Distances (Å)			
Ir–P(1)	2.390(2)	Ir–Cl(1)	2.379(2)
Ir–P(2)	2.385(2)	Ir–Cl(1A)	2.402
Ir–C(61)	1.878(8)	Ir–C(1)	2.190(9)
Ir–C(61A)	1.85	Ir–C(2)	2.156(8)
O(1)–C(9)	1.434(12)	O(5)–C(26)	1.52(4)
O(1)–C(10)	1.452(11)	O(5)–C(27)	1.41(4)
O(2)–C(7)	1.494(14)	C(6)–C(19)	1.35(7)
O(2)–C(8)	1.447(14)	C(6)–C(20)	1.38(7)
O(3)–C(11)	1.45(4)	O(7)–C(4)	1.39(6)
O(3)–C(28)	1.46(4)	O(7)–C(3)	1.53(6)
O(4)–C(5)	1.46(4)		
O(4)–C(6)	1.51(3)		
Angles, deg			
P(1)–Ir–P(2)	112.88(8)	Cl(1)–Ir–C(61)	176.4(3)
C(1)–Ir–C(2)	40.4(3)	P(1)–Ir–C(61)	85.5(3)
P(1)–Cl(1)	91.59(8)	P(2)–Ir–C(61)	92.6(3)
P(2)–Cl(1)	86.49(9)	P(1)–Ir–C(61)	85.5(3)
C(9)–O(1)–C(10)	62.9(6)	P(2)–Ir–C(61)	92.6(3)
C(7)–O(2)–C(8)	57.7(6)	C(27)–O(5)–C(26)	57(2)
C(11)–O(3)–C(28)	58(2)	C(19)–O(6)–C(20)	62(3)
C(5)–O(4)–C(6)	56.6(11)	C(4)–O(7)–C(3)	58(3)

carbonyl, chloride, and phosphine ligands on the iridium have the expected arrangement. Bond distances and angles within this unit are in the expected ranges. However, there is severe disorder in the locations of the oxygen atoms. For  $(\eta^2-C_{60}O_2)Ir(CO)Cl(PPh_3)_2 \cdot 5C_6H_6$  there are seven oxygen sites with fractional occupancies as follows: O(1), 0.761(14); O(2), 0.500(12); O(3), 0.159(12); O(4), 0.224(12); O(5), 0.148(12); O(6), 0.089(12); and O(7), 0.093(12). The locations of each of these sites are similar. In each case the oxygen atoms lie over 6:6 ring junctions, and the geometries within each unit are consistent with the presence of epoxide functionalities on the fullerene core. In addition to the disorder in the location of the oxygen atoms, there is exchange disorder in the positions of the carbonyl and chloride ligands that are bound to iridium. The relative occupancies are 0.836(9) for the chloride ligand at site Cl(1) as shown in Figure 6 and 0.164(9) for the site Cl(1A) which occupies a position between C(61) and O(10) of the carbon monoxide ligand. This sort of exchange disorder between a carbon monoxide ligand and a chloride ligand is common in Vaska's compound<sup>29</sup> and complexes made from it.<sup>11,21</sup>

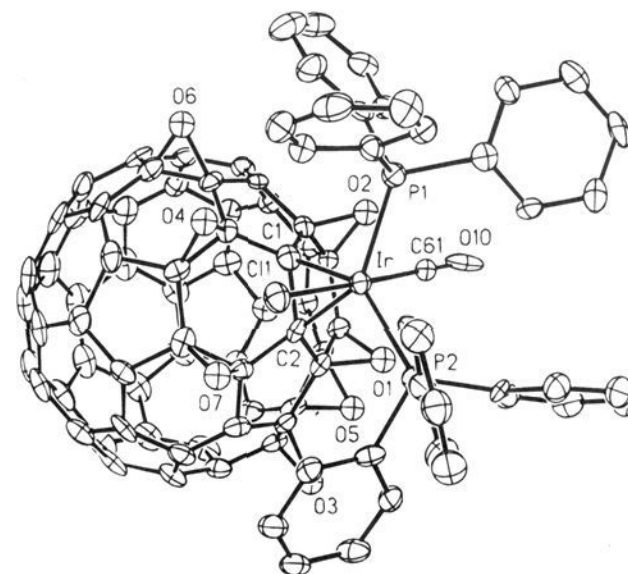


**Figure 6.** A drawing (with 50% thermal contours) of the molecular structure of  $(\eta^2-C_{60}O_2)Ir(CO)Cl(PPh_3)_2$  which shows the positions of all seven partially occupied oxygen sites. Those fractional occupancies are as follows: O(1), 0.761(14); O(2), 0.500(12); O(3), 0.159(12); O(4), 0.224(12); O(5), 0.148(12); O(6), 0.089(12); and O(7), 0.093(12). For the exchange disordered chloride and carbon monoxide ligands only the major orientation is shown.

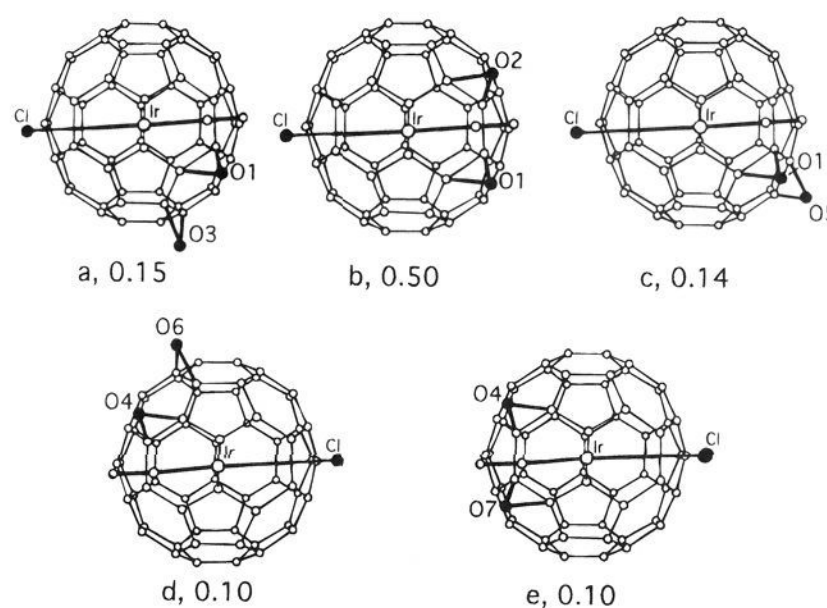


**Figure 7.** Drawings of the five forms of  $(\eta^2-C_{60}O_2)Ir(CO)Cl(PPh_3)_2$  in the specific orientations that occupy a common site in the solid state and produce the disorder in the locations of the epoxide groups and the chloride and carbon monoxide ligands. For clarity, the locations of the phenyl rings have been omitted from these drawings.

Although the disorder problems are serious, the pattern of occupancies of these sites can be analyzed to determine which of the isomers of  $C_{60}O_2$  is actually present in the crystal. Notice the high occupancies of sites O(1) and O(2), which are adjacent to one another on a common six-membered ring. This arrangement suggests that the  $C_s$  isomer **H** in Figure 5 is present. The results of further analysis are shown in Figure 7. This figure presents drawings of the five forms of the complex that occupy a common position and therefore are involved in the observed disorder. For clarity, the positions of the triphenylphosphine ligands, which are common to all five forms, have been omitted in these drawings. The fractional occupancy of each form is given below each individual drawing. This analysis involves the following suppositions. Only a single  $C_{60}O_2$  isomer, isomer **H** in Figure 5, is present. The positions of the carbon monoxide and chloride ligands and the oxygen atoms on the fullerene are correlated so that a carbon monoxide ligand, and not a chloride ligand, is adjacent to an epoxide function. This minimizes contact between the ligand and the epoxide unit and places the smaller ligand next to the epoxide portion. The model shown

(29) Churchill, M. R.; Fetting, J. C.; Buttrey, L. A.; Barkan, M. D.; Thomson, J. S. *J. Organomet. Chem.* **1988**, 340, 257.

in Figure 7 results in the following occupancies: O(1), 0.79; O(2), 0.50; O(3), 0.15; O(4), 0.20; O(5), 0.14; O(6), 0.10; O(7), 0.10; and Cl, 0.80. These values are in good agreement with the observed occupancies. No arrangement that utilizes the other two  $C_s$  isomers of  $C_{60}O_2$  can adequately explain the observed pattern of fractional occupancies within this solid. This statement is best justified by considering how pairs of oxygen atom sites relate to the oxygen atom locations required by the isomers **D** and **G**. Isomer **D** alone cannot be present, since only the pair of oxygen sites O(4) and O(5) has the mutual juxtaposition that is required for the presence of this isomer. For isomer **G** the following pairs of oxygen atoms have the proper mutual orientation: O(1) and O(7), O(2) and O(4), O(2) and O(5), O(2) and O(6), and O(3) and O(7). However, within these pairs there are severe problems in attempting to account quantitatively for the occupancies of the seven sites. The problem is greatest at the highest occupancy site, O(1). This site, with an occupancy of 0.761, is paired only with site O(7) which has a much lower occupancy, 0.093, and there is no way that this model can account for the high occupation of site O(1). Moreover, the low occupancy site O(7) is also linked with site O(3) which has an occupancy of 0.159, a value which is again greater than the occupancy at site O(7).

### Discussion

Experience in this laboratory indicates that the *m*-chloroperoxybenzoic acid oxidation of  $C_{60}$  is the preferred method of generating both  $C_{60}O$  and  $C_{60}O_2$ , although chromatographic separation of the products is required and can be quite tedious. The chromatographic separation described here yields  $C_{60}O_2$  as a single isomer along with other products which have yet to be identified. Since this work was completed, a brief report on the *m*-chloroperoxybenzoic acid oxidation of  $C_{60}$  has appeared.<sup>30</sup> The  $^{13}C$  NMR spectrum of  $C_{60}O_2$  reproduced in that article is substantially similar to the spectrum shown in Figure 3, although detailed comparison of the region from 141 to 147 ppm is hampered by the compressed scale used in ref 30. We have re-examined the *m*-chloroperoxybenzoic acid oxidation of  $C_{60}$  under the conditions described in ref 30 but cannot obtain the yields that they claim to have obtained with a reaction using only 2 equiv of oxidant at room temperature.

Structural characterization of the one isomer of  $C_{60}O_2$  that has been purified has required both the use of  $^{13}C$  NMR spectroscopy and X-ray structural analysis of the crystalline adduct that is formed with Vaska's compound. Neither technique alone would have fully and unambiguously revealed the structure of  $C_{60}O_2$ . Disorder in the crystal structure of  $(\eta^2-C_{60}O_2)Ir(CO)Cl(PPh_3)_2 \cdot 5C_6H_6$  is a severe problem. However, modern computational methods allow the analysis of such data, and the value of these imperfect data must be recognized.

The structural data indicate that the most abundant higher oxide, isomer **H** of  $C_{60}O_2$ , retains the fullerene core intact. In this molecule the two epoxide units are as close to one another as possible. Their relative orientation is similar to what is observed with  $C_{60}H_4$  where the four hydrogen atoms radiate from a common hexagonal face.<sup>31</sup> Previous experimental work<sup>13</sup> as well as computational studies<sup>9</sup> have suggested that addition of two oxygen atoms to  $C_{60}$  would result in rupture of the fullerene cage. For the most abundant isomer of  $C_{60}O_2$ , no rupture of the cage has occurred.

$C_{60}O_2$  binds Vaska's complex in positions that place the metal complex near the epoxide units, but the addition reaction does

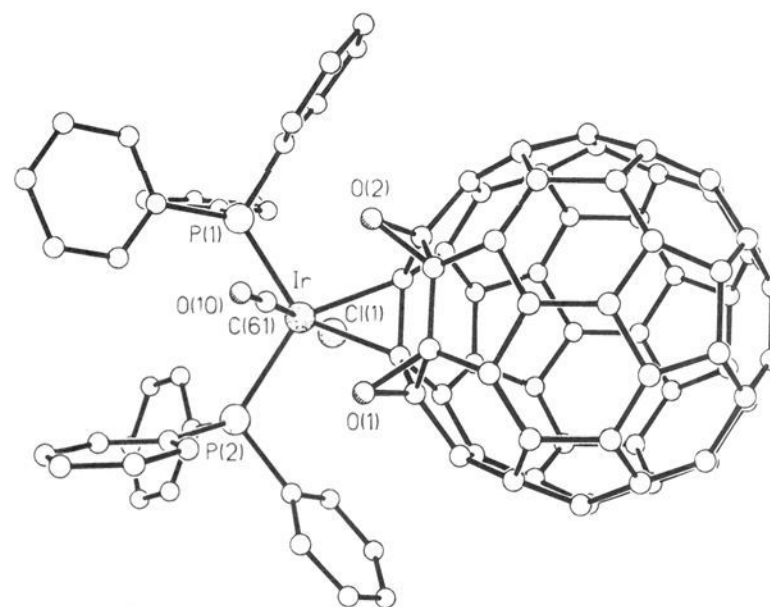


**Figure 8.** A drawing of the major form, b, of  $(\eta^2-C_{60}O_2)Ir(CO)Cl(PPh_3)_2$ . Except for the positions of the phenyl rings and the orientation within the crystal, forms b and e, which account for 60.3% of the molecules present in the solid, have this geometry.

leave the epoxide units intact. In contrast, there are a number of reactions known in which a low oxidation state metal complex inserts itself into the C–O bond of an epoxide.<sup>32,33</sup> That does not occur here. The positioning of the iridium complex on the fullerene surface is similar to what is seen with  $(\eta^2-C_{60}O)Ir(CO)Cl(PPh_3)_2$  where the epoxide and the iridium complex are attached to a common hexagonal face of the fullerene oxide. In the crystalline state of  $(\eta^2-C_{60}O_2)Ir(CO)Cl(PPh_3)_2$  there are three isomeric molecules that result from the relative locations of the epoxide and iridium units. While Figure 7 shows that five forms of  $(\eta^2-C_{60}O_2)Ir(CO)Cl(PPh_3)_2$  are present, two, b and e, have the same geometry as the  $(\eta^2-C_{60}O)Ir(CO)ClP_2$  unit and differ only in their orientation in the solid and the arrangement of the phenyl rings with respect to the rest of the structure. Figure 8 shows a drawing of the major form, b. In this form and in e as well, the carbon monoxide ligand bisects the space between the two epoxide units. Two other forms, a and d, represent a second isomer where the iridium complex is attached to a different site of the fullerene diepoxide. Again these two forms differ only in the relative positioning in the crystal site and in the arrangement of the phenyl rings. With the a and d forms, the iridium complex is bound not to the hexagonal face of the fullerene that contains the two epoxide units but to an adjacent hexagonal face. This places the iridium complex and one of the epoxide units on a common hexagon and also locates the iridium atom and the two oxygen atoms so that their positions radiate from a common pentagonal face. In these two forms there is less contact between the carbon monoxide ligand and the fullerene diepoxide than in forms b and e, since that ligand makes contact with only one of the epoxide units. This isomer is chiral. Since the crystal contains a center of symmetry, both enantiomers are present. The third form, c, also has the iridium and one epoxide unit occupying a common hexagonal face. Form c differs from forms a and d in the relative locations of the iridium atom and the two oxygen atoms. These three groups do not radiate from a common pentagonal face of the fullerene diepoxide as they do in forms a and d. In form c the distance between the iridium atom and the more remote epoxide unit is larger than it is in forms a and d. This isomer is also chiral, but due to the center of symmetry, both enantiomers are present. The presence of these three distinct isomers in the crystalline

(30) Ishida, T.; Tanaka, K.; Furudate, T.; Nogami, T.; Kubota, M.; Kurono, S.; Ohashi, M. *Fullerene Sci. Technol.* **1995**, 3, 85.

(31) Henderson, C. C.; Rholting, C. M.; Assink, R. A.; Cahill, P. A. *Angew. Chem., Int. Ed. Engl.* **1994**, 33, 786.

(32) Lenarda, M.; Ros, R.; Traverso, O.; Pitts, W. D.; Baddley, W. H.; Graziani, M. *Inorg. Chem.* **1977**, 16, 3178.

(33) Schlodder, R.; Ibers, J. A.; Lenarda, M.; Graziani, M. *J. Am. Chem. Soc.* **1974**, 96, 6893.

solid correlates well with the infrared spectral observation which shows the presence of three carbon monoxide stretching frequencies.

Formation of adducts between  $C_{60}$  and  $Ir(CO)Cl(PPh_3)_2$  is a reversible process, and that is also expected to be true of additions with the fullerene oxides. Co-crystallization of three isomers in the five forms seen in Figure 7 is a consequence of the similarity of the external shapes of these closely related molecules and entropic factors which favor disorder. As with binding of Vaska's complex and  $C_{60}O$ , there is an apparent thermodynamic preference for locating the iridium complex close to the epoxide units. The balance between placing the iridium complex immediately adjacent to both epoxide units in  $C_{60}O_2$ , as is the case for the most prevalent isomer (Figure 8), and steric factors, which are maximized in this isomer where the carbon monoxide ligand bisects the two epoxide units, probably is a factor in co-crystallization of the other two isomers.

### Experimental Section

**Preparation of Compounds.**  $C_{60}$  was prepared by the arc vaporization of graphite<sup>34</sup> and purified by column chromatography on alumina.

**Oxidation of  $C_{60}$  with *m*-Chloroperoxybenzoic Acid.** The *m*-chloroperoxybenzoic acid was purified by washing with pH 7.5 buffer before use.<sup>35</sup> A solution of *m*-chloroperoxybenzoic acid (135 mg, 0.79 mmol) in toluene (15 mL) was added with stirring to a heated solution of  $C_{60}$  (20 mg, 0.026 mmol) in toluene (15 mL) at 80 °C. The mixture was stirred for 1 h at 80 °C. After being cooled, the brown solution was evaporated to dryness under vacuum. The resulting brown solid was washed with two 4-mL portions of methanol. The remaining solid was then dissolved in a 30 mL of toluene. Separation and purification were performed by HPLC using the "Buckyclutcher 1" column with a 1:1 v/v mixture of toluene and *n*-hexane as the eluant. This procedure yielded  $C_{60}$  (peak 1, Figure 1, 10.9 mg, 60% yield),  $C_{60}O$  (peak 2, 6.9 mg, 30% yield), and  $C_{60}O_2$  (peak 4, 2 mg, 8% yield).

**Ozonolysis of  $C_{60}$ .** A 0.06-cfm dioxygen/ozone stream from a Welsbach ozonator, which was operated at 90 V ac, was passed through a solution that contained 4 mg of  $C_{60}$  in 10 mL of toluene. A nearly instantaneous color change from deep magenta to amber occurred upon introduction of the dioxygen/ozone vapor. After 1 min of contact with this vapor, the sample was subjected to 3 freeze-pump-thaw cycles to remove the ozone. The solution was stored under dinitrogen and analyzed by HPLC for several hours after the initial reaction. A representative example of these data is shown in Trace C of Figure 1. Over time, the relative proportions of the oxidation products in solution remained constant. However, a yellow-brown amorphous solid continued to precipitate from the solution until eventually the liquid portion was colorless.

**$(\eta^2-C_{60}O_2)Ir(CO)Cl(PPh_3)_2 \cdot 5C_6H_6$ .** Under a dioxygen-free atmosphere of dinitrogen, a filtered solution of 3 mg (4  $\mu$ mol) of  $C_{60}O_2$  in 1.5 mL of benzene was carefully layered over a filtered solution of 5 mg (6  $\mu$ mol) of  $Ir(CO)Cl(PPh_3)_2$  in 1 mL of benzene. The mixture was allowed to stand undisturbed for 7 days. The purple-black crystals that formed at the interface between the two solutions were collected by filtration and washed with cold benzene: yield 3 mg, 50% based on  $C_{60}O_2$ . Under microscopic examination the product appeared homogeneous and crystals suitable for X-ray crystallography were obtained.

**X-ray Data Collection.** A suitable crystal of  $(\eta^2-C_{60}O_2)Ir(CO)Cl(PPh_3)_2 \cdot 5C_6H_6$  was coated with a light hydrocarbon oil and mounted in the 130(2) K dinitrogen stream of a Siemens P4/RA diffractometer which was equipped with a locally modified LT-2 low-temperature device. Intensity data were collected with nickel filtered Cu K $\alpha$  radiation from a Siemens rotating anode X-ray generator that operated at 15 kW. Crystal data are given in Table 2. A linear decay of 14% in the intensities of two standard reflections was observed during the

**Table 2.** Crystal Structure Data

formula	$C_{127}H_{60}$	Z	4
	$ClIrO_3P_2$	$d_{calc}$ , $Mg \cdot m^{-3}$	1.591
$F_w$	1923.5	radiation, $\lambda$ (Å)	Cu K $\alpha$
color and habit	black plates	$\mu$ , $mm^{-1}$	(1.54178)
crystal system	monoclinic	range of transm factors	4.421
space group	$P2_1/n$	no. of data collected	0.52–0.89
<i>a</i> , Å	14.583(3)	no. of unique data	11317
<i>b</i> , Å	19.671(4)	no. of data refined	10465
<i>c</i> , Å	28.536(5)	no. of parameters	10464
$\alpha$ , deg	90	(restraints)	1142(4)
$\beta$ , deg	101.133(15)	$R$ ( $I > 2\sigma$ )	0.055
$\gamma$ , deg	90	$wR2$ (all data)	0.145
<i>V</i> , Å <sup>3</sup>	8032(3)		
<i>T</i> , K	130(2)		

week of data collection, and the data were scaled to adjust for this decay. The data were corrected for Lorentz and polarization effects. Further details are given in the supporting information.

**Structure Solution and Refinement.** Calculations were performed with SHELXTL Plus (Sheldrick, Siemens, 1990) and SHELXL-93 (Sheldrick, 1993). Scattering factors and corrections for anomalous dispersion were taken from a standard source.<sup>36</sup> An absorption correction was applied to the structures with the program XABS2 which calculates 24 coefficients from a least-squares fit of  $(1/A \text{ vs } \sin^2(q))$  to a cubic equation in  $\sin^2(q)$  by minimization of  $F_o^2$  and  $F_c^2$  differences.<sup>37</sup> The structure was solved in the space group  $P2_1/n$  with the use of direct and difference Fourier methods. Seven oxygen atom sites on the fullerene were identified. These were refined with a common thermal parameter, and their occupancies were allowed to vary. This refinement converged to the following values for the oxygen atom occupancies: O(1), 0.724(14); O(2), 0.473(12); O(3), 0.142(12); O(4), 0.208(12); O(5), 0.134(12); O(6), 0.075(12); O(7), 0.076(12) with a sum of 1.83 for the seven sites and a common thermal parameter of 0.026(2) Å<sup>2</sup>. In the final cycles of refinement the same procedure was used, but the seven occupancies were restrained to sum to 2.00(2) with the use of the SUMP routine of SHELXL-93. This procedure gave smooth convergence but resulted in a larger thermal parameter, 0.032(2) Å<sup>2</sup>, and the following oxygen occupancies: O(1), 0.761(14); O(2), 0.500(12); O(3), 0.159(12); O(4), 0.224(12); O(5), 0.148(12); O(6), 0.089(12); O(7), 0.093(12) with a sum of the occupancies of 1.97. The heights of these oxygen atom peaks ( $e \text{ \AA}^{-3}$ ) on a regular Fourier map are as follows: O(1), 6.73; O(2), 3.73; O(3), 1.93; O(4), 3.05; O(5), 2.07; O(6), 1.39; O(7), 2.07. The chloride and carbon monoxide ligands bound to iridium show exchange disorder. The relative occupancies were allowed to refine and converged to 0.836(9)/0.164(9). For the purposes of convergence, the oxygen and carbon thermal parameters of the minor component were fixed at 0.02 Å<sup>2</sup>, and their positions were fixed at the locations that were derived from the difference map. In addition, one of the molecules of benzene is disordered and was modeled with 0.70/0.30 occupancies of rigid six-membered rings. Hydrogen atoms were fixed to appropriate carbon atoms through the use of a riding model and isotropic thermal parameters equal to 1.2 times the equivalent isotropic thermal parameter of the adjacent carbon atom. Refinement involved full-matrix, least-squares methods based on  $F^2$  and with the use of all data. Anisotropic thermal parameters were used for all non-hydrogen atoms with the exclusion of the disordered benzene molecule and the minor components of the chloride and carbon monoxide ligands. The final difference map showed the following five most prominent features: two peaks of 1.6  $e \text{ \AA}^{-3}$  magnitude that were 1.3 Å from the iridium atom, a peak (0.90  $e \text{ \AA}^{-3}$ ) that is 0.90 Å from P(1), a peak (0.89  $e \text{ \AA}^{-3}$ ) that is 1.67 Å from C(61) and 1.67 Å from H(81), and a peak (0.88  $e \text{ \AA}^{-3}$ ) that is 1.19 Å from C(1), 1.37 Å from C(6), and 2.06 Å from Ir. The latter peak lies over a 5:6 ring junction of the fullerene. Careful examination of the fullerene surface in the difference map reveals two other small features over 5:6 ring junctions: a peak (0.52  $e \text{ \AA}^{-3}$ ) that is 1.61 Å from C(10), 1.64 Å from C(2), 2.61 Å from Ir; and a smaller feature (0.30  $e \text{ \AA}^{-3}$ ) that lies over the C(29)–C(46) ring junction. When these three small features

(34) Haufler, R. E.; Conceicao, J.; Chibante, L. P. F.; Chai, Y.; Byrne, N. E.; Flanagan, S.; Haley, M. M.; O'Brien, S. C.; Pan, C.; Xiao, Z.; Billups, W. E.; Ciufolini, M. A.; Hauge, R. H.; Margrave, J. L.; Wilson, L. J.; Curl, R. F.; Smalley, R. E. *J. Phys. Chem.* **1990**, *94*, 8634.

(35) Schwartz, N. N.; Blumberg, J. H. *J. Org. Chem.* **1964**, *29*, 1976.

(36) *International Tables for X-ray Crystallography*; D. Reidel Publishing Co.; Boston, MA, 1992; Vol. C.

(37) Parkin, S. P.; Moezzi, B.; Hope, H. *J. Appl. Cryst.* **1995**, *28*, 53.

over 5:6 ring junctions are included in the model as oxygen atoms, their unrestrained positions are less stable during refinement than those of the oxygen atoms O(1)–O(7), and the geometry that results is more skewed. Consequently, these features were assumed to be artifacts and were not included in our final model. There are no unusually short intermolecular contacts in the structure.

**Physical Measurements.** Infrared spectra were obtained from mineral oil (Nujol) mulls between KBr plates on a Mattson Galaxy FTIR 3000 spectrophotometer. The  $^{13}\text{C}$  NMR spectra were recorded on a General Electric QE-300 NMR spectrometer at 75.46 MHz with a pulse width of 6.0  $\mu\text{s}$ , an acquisition time of 1.16 s, and a delay time of 2 s. The solvent was carbon disulfide with 10% benzene- $d_6$  that was used for the internal lock. Chemical shifts were referenced internally to tetramethylsilane. Electronic spectra were recorded with a Hewlett-Packard 8450A spectrometer.

**Acknowledgment.** We thank the National Science Foundation (Grant CHE9321257) for support, Johnson Matthey Inc.

for a loan of iridium chloride, and Richard Koerner for assistance with the NMR measurements.

**Supporting Information Available:** Details of data collection and structure refinement, tables of atomic coordinates, bond distances and angles, anisotropic thermal parameters, and hydrogen atom positions for  $(\eta^2\text{-C}_{60}\text{O}_2)\text{Ir}(\text{CO})\text{Cl}(\text{PPh}_3)_2 \cdot 5\text{C}_6\text{H}_6$  (23 pages); listing of structure factor tables (24 pages). This material is contained in many libraries on microfiche, immediately follows this article in the microfilm version of the journal, can be ordered from the ACS, and can be downloaded from the Internet; see any current masthead page for ordering information and Internet access instructions.

JA9510065